Bioresource Technology 388 (2023) 129741

Contents lists available at ScienceDirect

Bioresource Technology

journal homepage: www.elsevier.com/locate/biortech

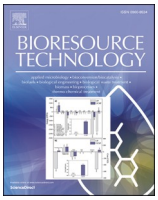

Production of (hydroxy)benzoate-derived polyketides by engineered *Pseudomonas* with *in situ* extraction

Tobias Schwanemann [a], Esther A. Urban [a], Christian Eberlein [b], Jochem Gätgens [a], Daniela Rago [c], Nicolas Krink [c], Pablo I. Nikel [c], Hermann J. Heipieper [b], Benedikt Wynands [a], Nick Wierckx [a,*]

[a] Institute of Bio- and Geosciences, IBG-1: Biotechnology, Forschungszentrum Jülich GmbH, Germany
[b] Department of Environmental Biotechnology, Helmholtz-Centre for Environmental Research - UFZ, 04318 Leipzig, Germany
[c] The Novo Nordisk Foundation Center for Biosustainability, Technical University of Denmark, Kongens Lyngby, Denmark

HIGHLIGHTS

- Heterologous production of benzoate-derived polyketides.
- Phenylpropanoids as reverse β-oxidation products from *Pseudomonas taiwanensis*.
- Production of fluorinated polyketides in a mutasynthesis approach.
- Solvent screening for efficient *in situ* product removal and boosted production.

GRAPHICAL ABSTRACT

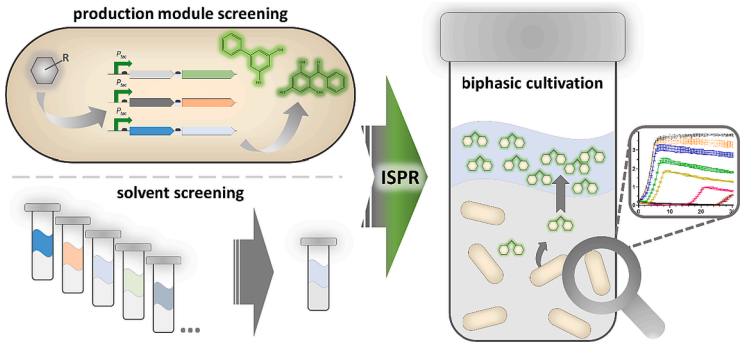

ARTICLE INFO

Keywords:
Benzophenones
Polyketide synthesis
Mutasynthesis
Pseudomonas taiwanensis
ISPR by extraction

ABSTRACT

Polyketides from (hydroxy)benzoates are an interesting group of plant polyphenolic compounds, whose biotechnological production is so far underrepresented due to their challenging heterologous biosynthesis. Efficient heterologous production of 2,4,6-tri- and 2,3′,4,6-tetrahydroxybenzophenone, 3,5-dihydroxybiphenyl, and 4-hydroxycoumarin by whole-cell biocatalysis in combination with *in situ* product extraction with an organic solvent was demonstrated. Production was highly dependent on the used CoA ligase and polyketide synthase type III. Therefore, different combinations of polyketide synthases and benzoate-CoA ligases were evaluated for their biosynthesis performance in the solvent-tolerant *Pseudomonas taiwanensis* VLB120. A solvent screening yielded 2-undecanone as biocompatible, extraction-efficient solvent with good phase separation. In aqueous-organic two-phase cultivations, this solvent extraction circumvents product instability in the aqueous cultivation medium, and it increases yields by reducing inhibitory effects. Complete *de novo* synthesis from glucose of all (hydroxy)benzoate-derived polyketides was achieved in two-phase cultivations with metabolically engineered strains. Additionally, mutasynthesis was applied to obtain fluorinated benzophenone derivatives.

* Corresponding author at: Institute of Bio- and Geosciences, IBG-1: Biotechnology, Forschungszentrum Jülich, Wilhelm-Johnen-Straße, 52425 Jülich, Germany.
E-mail address: n.wierckx@fz-juelich.de (N. Wierckx).

https://doi.org/10.1016/j.biortech.2023.129741
Received 27 July 2023; Received in revised form 5 September 2023; Accepted 6 September 2023
Available online 17 September 2023

1. Introduction

Plant secondary metabolites made by polyketide synthases type III (PKS III) (Morita et al., 2019) are a versatile group of compounds with diverse biosynthesis pathways and a high exploration potential for new compounds. Polyphenols made from coenzyme A (CoA)-activated phenylpropanoids, like stilbenoids or chalcones, are frequent targets of heterologous production in industrial biotechnology hosts (Isogai et al., 2022; Li et al., 2022) due to their applications as dietary and food supplements, as well as cosmetic ingredients (Kallscheuer et al., 2019). In contrast, polyketides synthesized by PKS III from smaller precursors like CoA-bound (hydroxy)benzoates are underrepresented in terms of their heterologous production. Ever since the first isolation of α-mangostin in 1849, plant-derived benzophenones and xanthones (Remali et al., 2022) have been an important source for dyes and phytoalexins with potential applications in the pharmaceutical sector and health-promoting effects (Bisht et al., 2021). In plants, biosynthesis of xanthones is achieved via the benzophenone synthesis pathway by benzophenone synthase (BPS), a PKS III. 2,4,6-Trihydroxybenzophenone (2,4,6-TriHBP), also known as phlorobenzophenone, is the C6 → C1 Claisen condensation product of the tetraketide intermediate, made from benzoyl-CoA and three malonyl-CoA by BPS. Benzophenones are themselves diverse secondary metabolites with large variety in glycosylation, prenylation, hydroxylation and other modifications (Beerhues & Liu, 2009; Wu et al., 2014). Access to these metabolites is so far limited to complex extraction from natural resources (Miller et al., 2020) or chemical synthesis (Ehianeta et al., 2016).

Due to these costly production processes and thus limited availability, the exploration of potential applications of these compounds is hindered. In order to circumvent laborious extraction processes of natural plant producers, underlying yield variation and seasonal variability, heterologous biosynthesis with microorganisms is a preferred approach to reliably provide the respective products in a sustainable manner (Kallscheuer et al., 2019; Prabowo et al., 2022). Additionally, the use of xenobiotic precursors allows the synthesis of synthetic analogues in mutasynthesis approaches (Reed & Alper, 2018). Halogenation with fluorine as substitute is often of interest during the development of pharmaceutical molecules because of altered persistence and accessibility while maintaining the desired biological activity (Cros et al., 2022). Conversion towards new-to-nature methyl- or fluorobenzophenones is not possible in the natural plant producer, but can be enabled through heterologous production in microbial hosts.

Heterologous microbial biosynthesis of polyketides can thus provide more efficient production and new-to-nature derivatives, but the product's antimicrobial activity and instability poses a major challenge (Virklund et al., 2022). Thus, an *ab initio* choice of a biotechnological production host with suitable native tolerance to the envisioned products and associated process conditions is essential to achieve efficient production (Blombach et al., 2022). Considering product-host-process interactions upfront, the genome-reduced solvent-tolerant *Pseudomonas taiwanensis* GRC3 (Wynands et al., 2019) was considered to be a suitable choice for investigating the heterologous biosynthesis of benzophenones and related compounds. This species has also been extensively engineered for the production of polyketide precursors including malonyl-CoA (Schwanemann et al., 2023), benzoate (Otto et al., 2020), *p*-coumarate (Wynands et al., 2023) and other aromatics (Schwanemann et al., 2020).

In this study, *P. taiwanensis* GRC3 was engineered for the production of 2,4,6-trihydroxybenzophenone, 2,3′,4,6-tetrahydroxybenzophenone, 3,5-dihydroxybiphenyl, 4-hydroxycoumarin, and new-to-nature derivatives thereof. This is achieved in an integrated approach including the selection and expression of efficient synthetic biosynthesis pathways, metabolic engineering for completely *de novo* production, feeding of precursor analogs in a mutasynthesis approach, and solvent selection for *in situ* product removal (ISPR) and stabilization. Through this approach the *P. taiwanensis* GRC3 platform was harnessed to facilitate production of highly interesting polyketides derived from benzoates and their derivatives.

2. Materials and Methods

2.1. Strains and cultivation conditions

All used strains in this study can be seen in the supplementary material. *Escherichia coli* DH5α and PIR2 were used as cloning hosts. Production experiments were performed with different strains of a genome-reduced *Pseudomonas taiwanensis* GRC3 (Wynands et al., 2019). *P. taiwanensis* VLB120, *Pseudomonas putida* KT2440, *E. coli* BL21 (DE3), *Bacillus subtilis* substrain 168, *Streptomyces venezuelae* NRRL B-65442 (DSM 112328), *Corynebacterium glutamicum* ATCC 13032 (DSM 20300), and *Saccharomyces cerevisiae* S288C (DSM 1333) were used in biocompatibility experiments. LB complex medium was routinely used during cloning and genetic engineering workflows and for seed cultures to inoculate minimal medium pre-cultures. Adaption cultures and production experiments were performed in Hartmans' mineral salt medium (MSM) with three-fold buffer concentration (3 * 22.3 mM K_2HPO_4 and 3 * 13.6 mM NaH_2PO_4) and 20 or 30 mM glucose, respectively (Schwanemann et al., 2023). Aromatic precursors or 180 μM cerulenin (resolved in methanol or ethanol) (Sigma-Aldrich) were supplemented from stock solutions. In biocompatibility experiments, other complex media, namely BHI medium (BD Difco™, United Kingdom), liquid GYM medium (glucose 4 g L^{-1}; yeast extract 4 g L^{-1}, malt extract 10 g L^{-1}) and YEPS medium (1% (w/v) yeast extract, 2% (w/v) peptone, 2% (w/v) sucrose) were used as indicated in the respective experiment for the respective species. If needed antibiotics were added (50 mg L^{-1} kanamycin sulfate; 20 mg L^{-1} gentamicin sulfate; 100 mg L^{-1} ampicillin sodium salt).

Cultivation in the presence of a second water-immiscible phase was performed in 4 mL ROTILABO glass sample vials in the Growth Profiler 960 (EnzyScreen, Heemstede, the Netherlands) with a white 3D-printed rack (Rönitz et al., unpublished). The filling volume was 500 μL MSM with three-fold buffer and 30 mM glucose with respective antibiotics, if needed. Use of different media is indicated in the respective experiments. Up to 20% (v/v) (i.e., 100 μL) solvents were added if solvents were used in subsequent HPLC analysis. In other solvent screening experiments (biocompatibility, carbon source, different organisms in the presence of 2-undecanone) 540 μL MSM and 60 μL solvent were used. Growth profiler settings were 30°C, 225 rpm with 50 mm amplitude and pictures were taken each 30 min and green values were obtained from the pixels by the corresponding software.

2.2. Plasmid and strain construction

New production strains of *P. taiwanensis* were either obtained by electroporation of replicating plasmids into twice with 10% (v/v) glycerol washed cell pellets (voltage 2500 V, capacitance 25 μF, resistance 200 Ω, cuvette 2 mm) or by site-specific genomic integration of mini-Tn7 transposons into the respective attachment site (Schwanemann et al., 2023). Plasmids were cloned applying the Gibson assembly methodology using the NEBuilder HiFi DNA Assembly Master Mix (New England Biolabs, New Ipswich, USA). All used plasmids, oligonucleotides and DNA fragments in this study can be seen in the supplementary material. PCRs and colony PCR were made using either Q5 polymerase or OneTaq polymerase with prior alkaline PEG lysis as described previously (Schwanemann et al., 2023).

2.3. Solvent screening, extraction and emulsification experiments

For the determination of extraction coefficients of 2,4,6-TriHBP, benzoate, cinnamate and flaviolin with different solvents, a solution of three-fold-buffered ultra-pure water was prepared to mimic the medium conditions with a concentration of approximately 1 mM of the respective

compound. A flaviolin solution was obtained from culture supernatant in three-fold buffered MSM of strain GRC3Δ6MC-II *attTn7*::*FRT-P*$_{14f}$-*SgRppA* (Schwanemann et al., 2023). Extraction was assessed at pH ~ 7 and 6.5. The pH was adjusted from 7.02 to 6.50 for 2,4,6-TriHBP, from 7.00 to 6.49 for benzoate, from 7.00 to 6.50 for cinnamate and from 7.02 to 6.50 for flaviolin solution using a 5 M hydrochloric acid solution. Extraction was performed in 2-mL reaction tubes in triplicates with different organic solvents and as a control without any solvent. Five-hundred microliter of the respective solvent and 500 μL of the respective aqueous solution were shaken at 1400 rpm for 10 min, centrifuged at 16,000 g for 10 min and finally the separate phases were analyzed for the compounds' concentration by HPLC.

For the extraction of 2,4,6-TriHBP with 1-octanol, a solution of ultrapure water with ~ 1 mM 2,4,6-TriHBP was prepared. The pH value was set between 4.1 and 10.1 with sodium hydroxide and hydrochloric acid solutions. Extraction was performed in 2-mL reaction tubes in triplicates. Except for the controls, 1 mL 1-octanol was added to 1 mL sample. The pH of the aqueous phase for each sample was measured in equilibrium. Phases were separately analyzed for 2,4,6-TriHBP concentrations by HPLC. Back-extraction experiments using 2-undecanone were performed analogously.

To investigate interphase formation of solvents with MSM and cells, strain GRC3Δ6MC-II was inoculated at higher cell density to OD_{600} 10.8. One milliliter of culture was transferred to a 2-mL reaction tube, as well as 500 μL of the respective solvent. The tubes were shaken at 1400 rpm for 13 h at room temperature. For visual comparison of phase separation and interphase formation, images were taken after shaking, centrifugation at 4000 g at 25 °C for 1.5 min, and after centrifugation for 6.5 min (see supplementary material). Variations of cell density and centrifugations are indicated in the respective experiments.

2.4. Sampling from production experiments and analytical methods

Determination of the optical density were performed at 600 nm with GE Healthcare Ultrospec™ 10 device from Fischer Scientific GmbH (Schwerte, Germany).

For regular cultivations in the Growth Profiler using 96-square-well plates with a filling volume of 200 μL, the obtained green value were converted to OD_{600} equivalents using the following calibration:

$$OD_{600}\ \text{equivalent} = a * (gValue - gBlank)^b + c * (gValue - gBlank)^d + e * (gValue - gBlank)^f.$$

with a = 0.0328, b = 1.08, c = 5.6 * 10^{-7}, d = 3.13, e = 1.47 * 10^{-13}, f = 6.64 and gBlank = 17.330. Abbreviations: gValue, green value; gBlank, green value of reference medium. The calibration was performed for the *P. taiwanensis* VLB120 wild type in half-deepwell microtiter plates (CR1496dg, EnzyScreen) sealed with sandwich covers (CR1296c, EnzyScreen).

2.4.1. GC-FID analysis of fatty acid composition

Extraction of membrane lipids was performed by an established procedure (Bligh & Dyer, 1959). The resulting fatty acid methyl esters (FAME) were analyzed by gas chromatography (GC) with flame ionization detector (FID) (Agilent Technologies 6890 N Network GC Systems; Model: HP5890, Hewlett-Packard, Palo Alto, USA). The used column was a 50 m CP-Sil 88 (Agilent Technologies) with 0.25 mm inner diameter and 0.25 μm film thickness. Helium flow was set to 1 mL min^{-1}. The GC temperature program started at 40°C for 2 min, followed by a temperature ramp of + 8 °C min^{-1} up to 220°C, which was hold for 5 min. The pressure program started at 27.7 psi (186.15 kPa) for 2 min, followed by a gradient of 0.82 psi min^{-1} (5.65 kPa min^{-1}) to final 45.7 psi (310.26 kPa) which was hold for 15.55 min. Injection temperature was 240°C with split-less injection volume of 1 μL by Agilent Technologies 7683B Series Injector, the FID detector temperature was 270°C. FAME were identified by co-injection of authentic reference compounds obtained from Supelco (Bellefonte, PA). *Trans/cis* ratio of unsaturated membrane fatty acids was calculated taking the sum of the FAME of palmitoleic acid (C16:1Δ9*cis*) and *cis*-vaccenic acid (C18:1Δ11*cis*) as divisor and the sum of their corresponding *trans* configuration as dividend (Heipieper et al., 1992).

2.4.2. Sample preparation from production experiments

Supernatant samples were made by centrifugation and subsequent filtration. To obtain extracts for polyketide analysis, 950 μL culture broth were transferred in a reaction tube with 50 μL 1 M hydrochloric acid. Then 950 μL ethyl acetate were added and vortexed for 15 min, followed by centrifugation and transfer to amber HPLC vials for evaporation as published previously by Schwanemann et al., (2023). Dried samples were resolved in acetonitrile for analysis in amber vials with PTFE-lined caps. From two-phasic cultivations, the cultivation tubes were centrifuged for 1 min at 4000 g and 50 μL of the organic layer were transferred into amber vials with an inlet for small volumes and measured in HPLC. Aqueous supernatants were obtained from filtered aqueous phase.

2.4.3. HPLC analysis

HPLC analysis was done as previously reported by Schwanemann et al., (2023) for the flaviolin acquisition method in 1260 Infinity II HPLC equipped with a 1260 DAD WR (Agilent Technologies) using an ISAspher 100-5 C18 BDS column (Isera, Düren, Germany) at a temperature of 30°C and a flow of 0.8 mL min^{-1}. Benzoate was detected at 232 nm after 9.47 min; 2,4,6-trihydroxybenzophenone at 330 nm after 11.43 min; cinnamate at 270 nm after 11.72 min; 3,5-dihydroxybiphenyl at 250 nm after 12.06 min. 3–hydroxybenzoate was detected after 6.75 at 300 nm, 3-hydroxycinnamate after 7.85 min at 270 nm and 2,3′,4,6-TetraHBP after 8.26 min at 330 nm. 2-Hydroxybenzoate (salicylate) was detected at 300 nm after 10.84 min and 4-hydroxycoumarin after 9.14 at 280 nm. 3-Methyl benzoate was detectable after 11.72 min at 232 nm.

Authentic standards were prepared in acetonitrile for 2,4,6-TriHBP, 2,3′,4,6-TetraHBP, 2,3-dihydroxybiphenyl and 4-hydroxycoumarin. Benzoic acids and phenylpropanoids were solved in water titrated with a sodium hydroxide solution if needed to obtain reference solutions.

2.4.4. GC-ToF MS analysis

Verification of sample composition was made for selected extraction samples by GC-ToF MS analysis according to a standard method published by (Hummel et al., 2010). Extract samples obtained from production experiments were resolved in acetonitrile which were previously used in HPLC analysis. The samples were lyophilized overnight in a Christ LT-105 freeze drier (Martin Christ Gefriertrocknungsanlagen, Osterode am Harz, Germany) and then stored at −20°C. Samples were consecutively derivatized with 50 μL MeOX (20 mg mL^{-1}O-methylhydroxylamine in pyridine) for 90 min at 30°C and 600 rpm in a thermomixer followed by an incubation with 80 μL of added MSTFA (N-acetyl-N-(trimethylsilyl)-trifuoroacetamide) for 90 min at 40°C and 600 rpm. For the determination of the derivatized metabolites an Agilent 6890 N gas chromatograph (Agilent, Waldbronn, Germany) was used coupled to a Waters Micromass GCT Premier high resolution time of flight mass spectrometer (Waters, Eschborn, Germany). The system was controlled by Waters MassLynx 4.1 software. Injections were performed by a Gerstel MPS 2 (Gerstel, Mülheim ad Ruhr, Germany) controlled by Maestro software. One microliter sample was injected into a split/splitless injector at 280°C at varying split modes.

The GC was equipped with a 30 m Agilent EZ-Guard VF-5 ms + 10 m guard column (Agilent, Waldbronn, Germany). The constant helium flow was set to 1 mL min^{-1}. The GC temperature program started at 60°C with a hold time of 2 min, followed by a temperature ramp of + 12 °C min^{-1} up to the final temperature of 300°C, hold time of 8 min.

The ToF MS was operated in positive electron impact $[EI]^+$ mode at an electron energy of 70 eV. Ion source temperature was set to 180°C. The MS was tuned and calibrated with the mass fragmentation pattern of Heptacosa (heptacosafluoro-tributylamine).

For the annotation of known metabolites, a baseline noise corrected fragmentation pattern together with the corresponding current RI value (Retention time Index) was compared to the in-house accurate *m/z* database JuPoD, and the commercial nominal *m/z* database NIST (National Institute of Standards and Technology, USA).

Unknown peaks were identified by a virtual reconstruction of the derivatized metabolite structure via the measured baseline noise corrected accurate mass *m/z* fragment pattern in comparison to an accurate *m/z* fragment register inside the JuPoD main library and were subsequent verified by virtual derivatization and fragmentation of the predicted structure.

2.4.5. LC-UV-MS/MS analysis

The analysis of mutasynthesis was done by LC-(UV)-MS/MS of culture supernatant and ethyl acetate extracts (prepared, as previously described for HPLC analysis).

The sample analysis was performed on a Vanquish Duo UHPLC binary system (Thermo Fisher Scientific, USA) coupled to a DAD-(ESI)IDX Orbitrap Mass Spectrometer (Thermo Fisher Scientific, USA), according to a previously published method (Kildegaard et al., 2021). Briefly, the chromatographic separation was achieved using a Waters ACQUITY BEH C18 (10 cm × 2.1 mm, 1.7 µm) equipped with an ACQUITY BEH C18 guard column kept at 40°C and mobile phase consisting of MilliQ water + 0.1% formic acid (A) and acetonitrile + 0.1% formic acid (B) using a flow rate of 0.35 mL min^{-1}. Sample injection was 1 uL. The DAD settings were 10 Hz for data collection rate and the wavelength range was 190–600 nm with a bandwidth of 2 nm.

The MS acquisition was set in positive and negative-heated electrospray ionization (HESI) mode with a voltage of 3500 V and 2500 V respectively, acquiring in full MS/MS spectra (Data dependent acquisition-driven MS/MS) in the mass range of 70–1000 Da. The data dependent acquisition settings were the following: automatic gain control (AGC) target value set at 4e5 for the full MS and 5e4 for the MS/MS spectral acquisition, the mass resolution was set to 120,000 for full scan MS and 30,000 for MS/MS events. Precursor ions were fragmented by stepped High-energy collision dissociation (HCD) using collision energies of 20, 40, and 60.

2.5. Statistical analysis

Analysis was performed by determination of the standard deviation (SD) or standard error of the mean (SEM) when indicated. In case of biological and technical replicates, the biological replicates were used for mean determinations. Additionally, ordinary one-way or two-way ANOVA with post-hoc tukey test using the software GraphPad Prism 9 with assumed Gaussian distribution, minimum $p < 0.05$ were applied when needed to determine significance.

3. Results and discussion

3.1. Toxicity and properties of 2,4,6-trihydroxybenzophenone and cellular response

Properties of benzoate-derived polyketides and physiological effects on biotechnological production hosts are still a mostly unexplored field. In order to gain a solid basis for heterologous natural product formation, the toxicity of 2,4,6-TriHBP on an aromatics catabolism-deficient *Pseudomonas taiwanensis* GRC3Δ6 (Δ*pobA*, Δ*hpd*, Δ*quiC*, Δ*quiC1*, Δ*quiC2*, Δ*benABCD*) was investigated using different concentrations of 2,4,6-TriHBP (Fig. 1A). With increasing concentrations of 2,4,6-TriHBP the biomass formation decreased with a correlating prolonged lag phase. The decreasing biomass in dependency to the applied 2,4,6-TriHBP

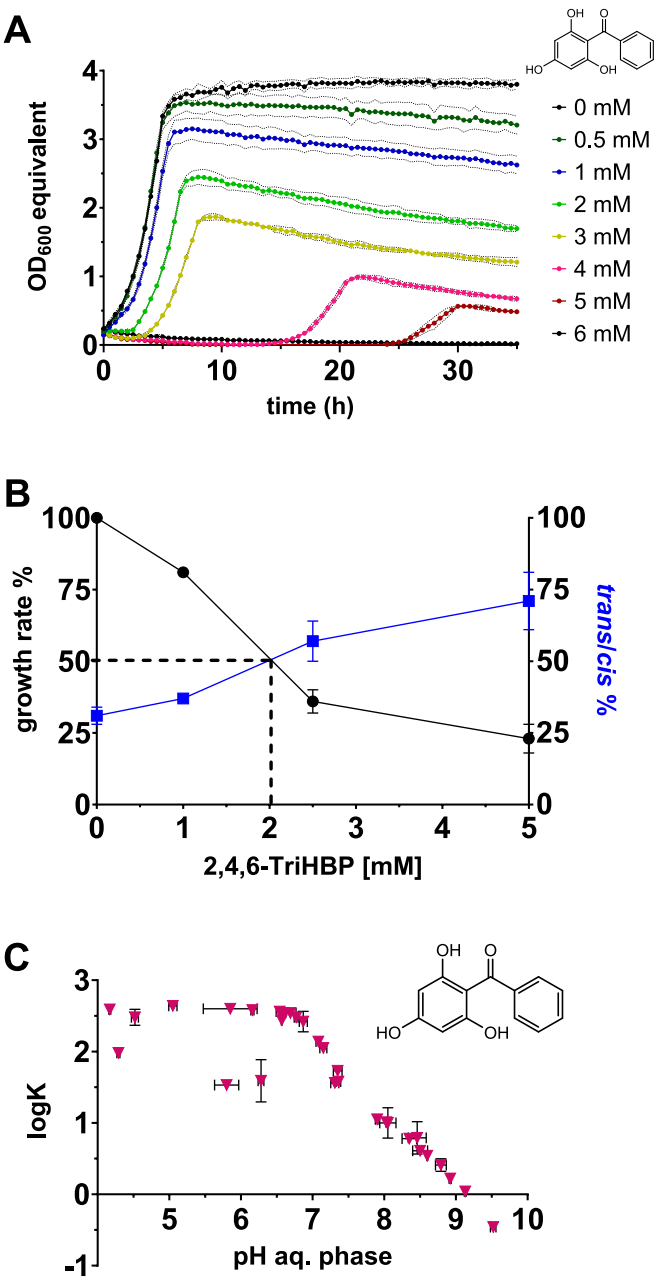

Fig. 1. Characterization of 2,4,6-TriHBP effects on host organism and partitioning in buffer:1-octanol system. **A)** Growth of *P. taiwanensis* GRC3Δ6 in mineral salt medium (MSM) with 20 mM glucose and 2,4,6-TriHBP (0–6 mM) in 96-square-well plate Growth Profiler cultivations (green value converted to OD_{600} equivalent) with initial OD_{600} 0.2. **B)** Relative growth rate from OD_{560} and *trans/cis* ratio of membrane phospholipids of *P. taiwanensis* GRC3 grown in MSM with 10 mM succinate in dependence to added 2,4,6-TriHBP. Error bars represent the standard deviation of the mean ($n_{bio} = 2$, $n_{tech} = 3$). The dashed line represents the IC_{50} concentration. **C)** Logarithmic plot of the partitioning coefficient of an aqueous 2,4,6-TriHBP solution (170 mg/L) containing 36 mM phosphate buffer with 1-octanol in 1:1 mixtures in dependence of the pH in equilibrium (pH 4.17 to 9.52). The pH was adjusted with 0.1 M HCl_{aq} and $NaOH_{aq}$ at 25°C. Error bars represent the standard deviations of the pH and $logK_{O/W}$ (n = 3, if not indicated differently).

concentration is an indication of 2,4,6-TriHBP uncoupling the proton motive force or of an energy-demanding tolerance mechanism of the microorganism. Interestingly, the biomass signal of the control culture with no 2,4,6-TriHBP stayed nearly constant over the whole period of cultivation, while biomass values decreased over time in the stationary

phase of cultures supplemented with 2,4,6-TriHBP. In addition, a red colorization of the cultures and the medium controls was observed, which could also influence the green pixel counts (green value) of the Growth Profiler which were converted into OD_{600} equivalents. Thus, the decrease in the stationary phase could either result from cell lysis and/or counteracting pixel readouts from ongoing color change. The 2,4,6-TriHBP concentration was strongly reduced at the end of cultivation in both medium controls and culture supernatants (see supplementary material). Therefore, toxicity might be exacerbated by as yet unknown degradation products of 2,4,6-TriHBP.

In order to examine toxicity effects of 2,4,6-TriHBP itself, 2,4,6-TriHBP was spiked directly into exponentially growing cultures of *P. taiwanensis* VLB120 wild type and GRC3 on succinate. The toxicity given as the effective concentration (EC_{50}) causing 50% growth inhibition was determined and, additionally, cellular phospholipids were extracted and analyzed for their *trans/cis* fatty acids composition. This composition allows to draw conclusions of the activity of the periplasmic *cis–trans*-isomerase (Cti) (Eberlein et al., 2018) and thus the mode of toxicity of 2,4,6-TriHBP. The graphically determined EC_{50} of *P. taiwanensis* GRC3 was approximately 2 mM (Fig. 1B) and 2.3 mM for the wild type (see supplementary material). This is in a similar range compared to other compounds with a similar $LogP_{O/W}$ like toluene and 4-chlorophenol. The *trans/cis* ratio of unsaturated fatty acids shifted from 0.31 to 0.37, 0.57 and up to 0.71 with the increasing applied 2,4,6-TriHBP concentrations in strain GRC3. This indicates activity of the short-term stress response deriving from Cti which has only access to its substrates when the inner membrane stability is impaired due to changes in its fluidity and rigidity, and thus its permeability (Eberlein et al., 2018). Thus, 2,4,6-TriHBP is directly affecting the bacterial inner cell membrane rigidity which likely contributes to its cytotoxicity. In contrast to the prior toxicity experiment (Fig. 1A), the later supplementation and quantification of the effects in growth and fatty acid composition allows to subscribe the observed effects directly to 2,4,6-TriHBP.

The partitioning of small uncharged compounds into biological membranes correlates with their partitioning coefficient of water and octanol ($logP_{O/W}$) (Heipieper et al., 2007). Therefore, partitioning of 2,4,6-TriHBP was tested at different pH values in an octanol–water system. Due to the definition of $logP_{O/W}$ as pure water-octanol mixture, the values obtained here are given as $logK_{O/W}$ due to the presence of salts in the aqueous phase (Fig. 1C). 2,4,6-TriHBP partitioning into octanol decreased with increasing pH due to its deprotonation. At acidic conditions up to a pH of approximately 6.5, the $logK_{O/W}$ remains constant at ~ 2.6 and the solution remains transparent. From pH 6.5 to 9 distribution shifted towards equal partitioning ($logK_{O/W} \approx 0$) until it is predominantly present in the aqueous phase at pH > 9 and yellow colored in the aqueous phase. This pH-dependent partitioning may result in interference of the proton motive force and thus contribute to the toxic properties of 2,4,6-TriHBP because compounds with a $logP_{O/W}$ of 1–5 are generally considered as toxic due lethal accumulation in bacterial membranes if their water solubility is sufficient (Schwanemann et al., 2020). Many natural small-size products are within this toxic range (Schönsee & Bucheli, 2020) contributing to their challenging high titer production in biotechnological hosts.

3.2. Identification of suitable enzyme combinations for benzoate polyketide synthesis

For biosynthesis of benzophenones and related polyketides, a respective aromatic precursor has to be CoA-activated by a ligase and subsequently converted by a BPS or biphenyl synthase (BIS). In order to identify suitable combinations of these two activities, pBT7T plasmid-based expression of different benzoate-CoA ligases and BPS or BIS were screened in *P. taiwanensis* GRC3Δ6. This screening was done in biotransformation experiments with high initial biomass and cerulenin as fatty acid biosynthesis inhibitor to artificially increase malonyl-CoA supply, which revealed a production dependence on the used ligase and BPS (Fig. 2). The combination of BPS from *Hypericum sampsonii* (HsBPS) and benzoate-CoA ligase from *Rhodopseudomonas palustris* (RpBZL) performed significantly the best for 2,4,6-TriHBP formation, achieving a titer of 270 ± 3 mg L^{-1} (Fig. 2A). Biosynthesis of 2,4,6-TriHBP was previously demonstrated in *Escherichia coli* without providing quantitative data (Klamrak et al., 2021). Another study using *Saccharomyces cerevisiae* achieved approximately 450 µg/L of 2,4,6-TriHBP from glucose and supplemented benzoate (Liu et al., 2020). In both cases, heterologous biosynthesis was likely limited by product stability and toxicity, precursor supply, as well as enzyme expression and activity (Virklund et al., 2022). Therefore, the here shown combinatorial pathway screening in a tolerant host demonstrated its potential.

In plants, 2,3′,4,6-TetraHBP serves as universal precursor for xanthone biosynthesis (Beerhues & Liu, 2009) and is made either from 2,4,6-TriHBP by selective oxidation, or from 3-hydroxybenzoate as ligation substrate (Remali et al., 2022). For the formation of 2,3′,4,6-TetraHBP from 3-hydroxybenzoate combinations of HaBPS or HsBPS with ligases RpBZL or $PxBCL_M$ performed similarly well in our experimental setup without significant difference (Fig. 2B). This exploitation of substrate promiscuity led to much lower titers of 26–27 mg L^{-1}, but this first heterologous 2,3′,4,6-TetraHBP synthesis was confirmed by GC-ToF MS (see supplementary material) and by an authentic reference standard in HPLC.

Benzoate-derived polyketide aromatic ring formation can also be achieved by an aldol condensation reaction, catalyzed by BIS resulting in formation of 3,5-dihydroxybiphenyl, a precursor of the phytoalexin aucuparin (Beerhues & Liu, 2009; Liu et al., 2007). GC-TOF was applied (see supplementary material) to confirm the formation of 3,5-dihydroxybiphenyl from benzoate with ligase RpBZL in combination with BIS1 from *Malus domestica* (MdBIS1) at low titers (Fig. 2C). This indicates a lower activity of BIS compared to BPS in heterologous application.

Interestingly, in all these biotransformation cinnamate or 3-hydroxycinnamate were identified as by-product, in accordance with the applied precursor benzoate or 3-hydroxybenzoate. These by-products did not occur when a PKS III was used that does not accept benzoyl-CoA as substrate like ScCHS, indicating that *in vivo* synthase activity was involved in their formation.

Some PKS III were reported to have a promiscuous activity for 4-hydroxycoumarin synthesis from salicyl-CoA (2-hydroxybenzoyl-CoA) and one malonyl-CoA (Liu et al., 2010). 4-Hydroxycoumarin is a natural precursor of anticoagulants and was thus of interest in previous metabolic engineering studies but not by exploiting BIS side-activity (Choo & Ahn, 2019; Lin et al., 2013). In the conversion approach of 2-hydroxybenzoate (salicylate) 4-hydroxycoumarin could be detected in small amounts in all approaches, revealing the applicability of BIS for its *in vivo* formation (Fig. 2D). The most suitable enzyme combination for that was BIS1 from pear *Pyrus communis* (PcBIS1) with CoA ligase SdgA from *Streptomyces sp*. WA46. In conclusion, each product was successfully biosynthesized and its identity confirmed. Additionally, a suitable combination for each product was identified by a biotransformation approach with cerulenin.

3.2.1. Characterization of selected polyketide production strains

After identification of suitable combinations of BPS/BIS with respective CoA ligases the conversion of the precursor towards the polyketide was done without the use of heavily interfering cerulenin in fatty acid biosynthesis to provide artificially high malonyl-CoA availability. Therefore, *P. taiwanensis* GRC3Δ6MC-II with increased malonyl-CoA availability and without benzoate degradation pathway was used for synthesis of benzoate-derived polyketides to allow direct comparison of the different production pathways.

Highest titers of about 59 ± 9 mg L^{-1} were achieved for 2,4,6-TriHBP from benzoate (Fig. 3A), while conversion with MdBIS1 resulted in about 1 mg L^{-1} 3,5-dihydroxybiphenyl (Fig. 3A). The relatively low production of 3,5-dihydroxybiphenyl is in line with reported *in vitro*

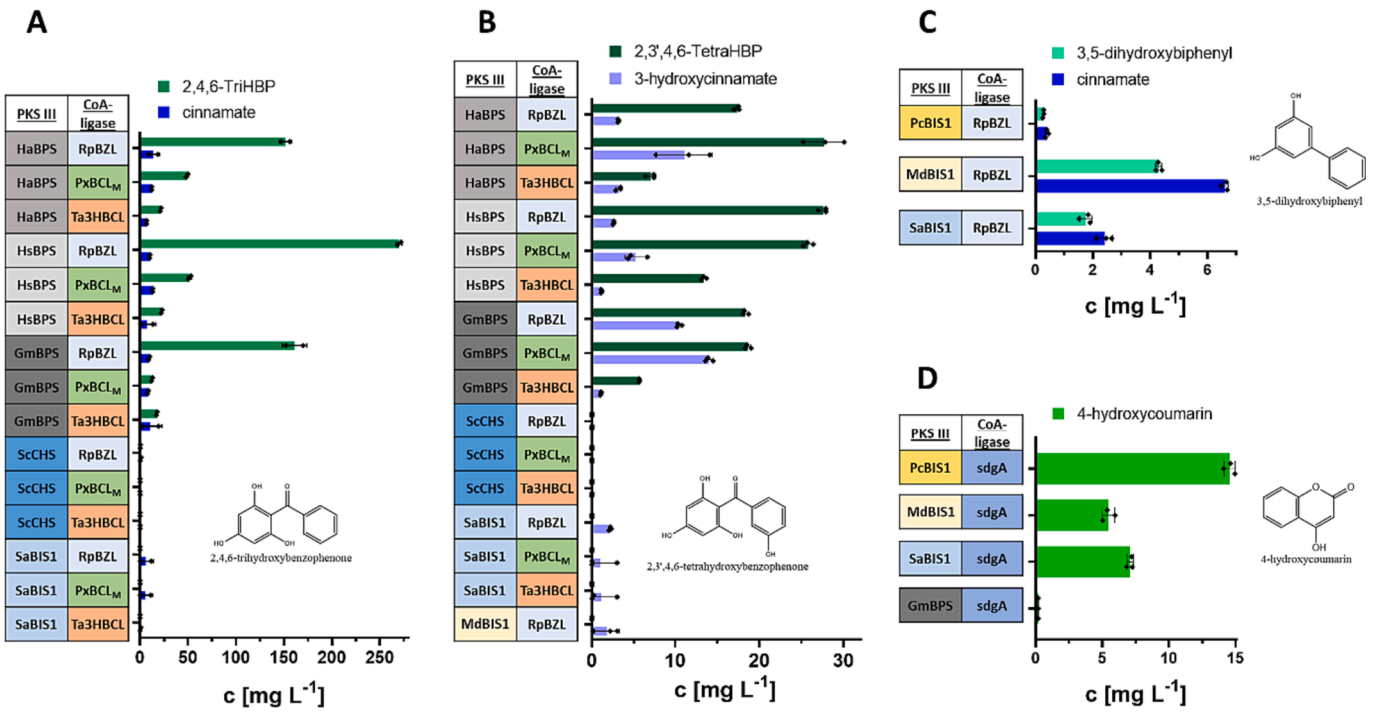

Fig. 2. Tested enzyme combinations for product synthesis by cerulenin supplemented transformations. **A**) Titers from biotransformation of benzoate to 2,4,6-TriHBP and cinnamate by different gene combinations expressed from pBT'T plasmid in *P. taiwanensis* GRC3Δ6 cultured with an initial OD_{600} of 4. Error bars indicate standard deviation of the mean (n = 2). **B**) Titers from biotransformation of 3-hydroxybenzoate to 2,3′,4,6-TetraHBP and 3-hdroxycinnamate. **C**) Titers of 3,5-dihydroxybiphenyl and cinnamate from benzoate. **D**) 4-Hydroxycoumarin from 2-hydroxybenzoate biotransformation by different gene combinations. All biotransformations were performed in MSM with 30 mM glucose, 2 mM supplemented benzoate, 3-hydroxybenzoate or 2-hydroxybenzoate, 154.2 mM ethanol (from cerulenin stock) and 180 μM cerulenin with initial OD_{600} 1 if not indicated differently. Samples were 2-fold concentrated for HPLC analysis. Error bars represent the standard deviation (n = 3) if not indicated differently. Significance was determined by two-way ANOVA with tukey test. Abbreviations: HaBPS, benzophenone synthase from *Hypericum androsaemum*; HsBPS, benzophenone synthase from *Hypericum sampsonii*; GmBPS, benzophenone synthase from *Garcinia mangostana*; ScCHS, chalcone synthase from *Swertia chirayita*; SaBIS1, biphenyl synthase 1 from *Sorbus aucuparia*; MdBIS1, biphenyl synthase 1 from *Malus domestica*;, PcBIS1, biphenyl synthase 1 from *Pyrus communis*; RpBZL, benzoate-CoA ligase from *Rhodopseudomonas palustris*; $PxBCL_M$, benzoate-CoA ligase from *Paraburkholderia xenovorans* LB400; Ta3HBCL, 4-hydroxy/3-hydroxybenzoate-CoA ligase from *Thaurea aromatica* K172; sdgA, 2-hydroxybenzoate-CoA ligase from *Streptomyces* sp. WA46.

enzyme kinetics for HsBPS (Huang et al., 2012) and MdBIS1 (Stewart et al., 2017). As above, cinnamate was detectable in small amounts in both conversions. The produced 2,4,6-TriHBP and cinnamate only cumulate to half of the consumed concentration of benzoate (Fig. 3B), indicating that product instability plays a significant role here.

Promiscuity-based synthesis of 2,3′,4,6-TetraHBP from 3-hydroxybenzoate achieved titers of approximately 18 mg L^{-1} (Fig. 3 A), with no clear preference for the three tested enzyme combinations as observed previously in the presence of cerulenin (Fig. 2B). Synthesis of 4-hydroxycoumarin with PcBIS1-sdgA yielded a titer of about 3.7 ± 2.3 mg L^{-1}, which is orders of magnitude lower compared to previous studies using PqsD as synthase (Choo & Ahn, 2019; Lin et al., 2013). Nevertheless, this demonstrates BIS usability for 4-hydroxycoumarin synthesis, especially because using PqsD as alternative promiscuous synthase in our *Pseudomonas* host resulted in low titers close to the limit of detection. In total, these approaches demonstrate production dependence on malonyl-CoA availability in cultures without cerulenin, enzyme activity of used BPS compared to BIS and *Pseudomonas* as superior host in this application compared to previous studies (Klamrak et al., 2021; Liu et al., 2020).

3.3. Phenylpropanoids as by-products

In experiments containing benzoate or 3-hydroxybenzoate as precursor, cinnamate and 3-hydroxycinnamate, respectively, were detected by HPLC and GC-ToF MS analysis (see supplementary material). Cinnamate was not identified as by-product of published BPS *in vitro* characterizations (Nualkaew et al., 2012) or in our experiments using a chalcone synthase which does not accept benzoyl-CoA as substrate (ScCHS, Fig. 2A). These two aspects indicate that the by-products result from the interaction of the applied PKS III or its catalyzed reaction with the native metabolism of *P. taiwanensis*. Possibly, the formation of phenylpropanoids results from the formation of a tetraketide intermediate formed by PKS III and subsequent conversion in *P. taiwanensis* VLB120 in a partly reversed β-oxidation from overlapping activities (Fig. 4A). A CoA-activated benzoate or derivative serves as starter unit for benzophenone or biphenyl synthesis. Malonyl-CoA units are subsequently condensed to elongate the carbon chain by two C atoms at a time. In order to yield cinnamic acid it is necessary to reduce the first keto group of the polyketide intermediate by a redox equivalent to a hydroxy group (reaction A), requiring a 3-hydroxyacyl-CoA dehydrogenase activity, followed by a double bond formation by releasing H_2O (reaction B) by an enoyl-CoA hydratase activity. Lastly, the phenylpropanoyl-CoA is hydrolyzed (reaction C) to obtain free phenylpropanoic acid and CoA. Alternatively, the last reaction could by catalyzed by a CoA-transferase or it could occur through spontaneous hydrolysis. A similar reversed β-oxidation has been described in different hosts (Kallscheuer et al., 2017). Interestingly, 4-hydroxycoumarin synthesis does not result in detectable 2-hydroxycinnamate formation but it is reported that this molecule can spontaneously form coumarin instead. The here observed phenomenon reveals the capability of *Pseudomonas* to utilize PKS III catalytic intermediates through one of its many complex β-oxidation pathways (Thompson et al., 2020). These findings open opportunities for promiscuous application of Pseudomonads' versatile metabolic capabilities for phenylpropanoid synthesis.

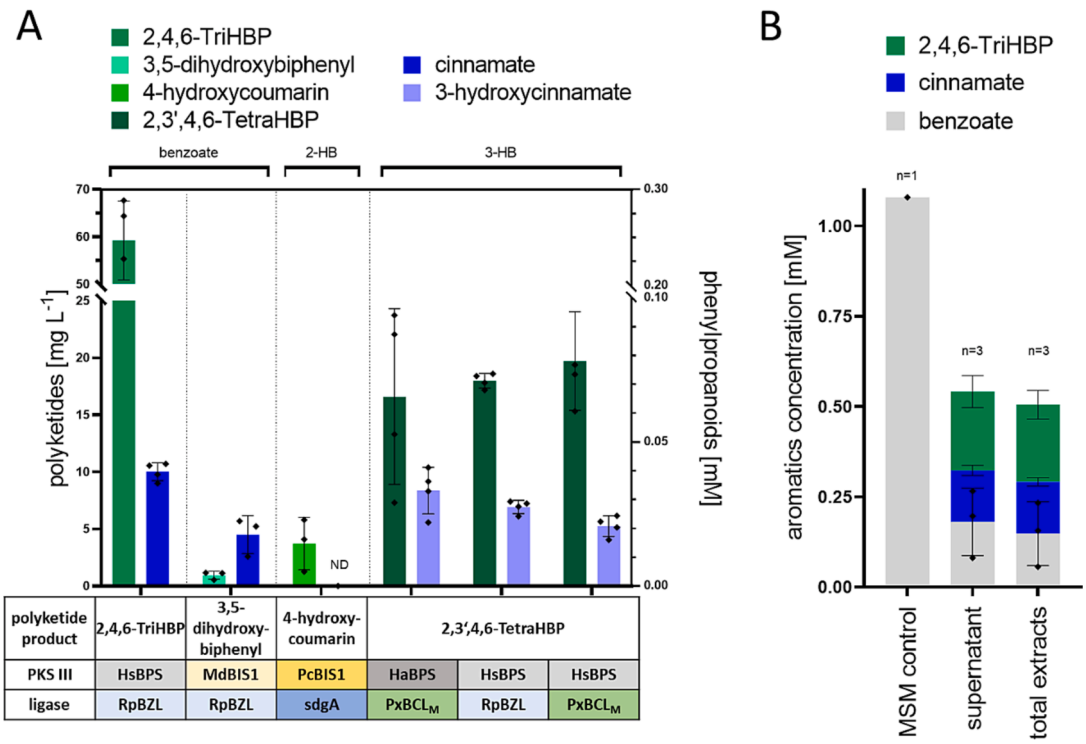

Fig. 3. Transformation and product stability with selected production strains. **A**) Titers of benzoate- and hydroxybenzoate-derived polyketides (green) and phenylpropanoid (blue) from respective supplemented precursors using platform strain GRC3Δ6MC-II with respective pBT'T plasmids. Inoculation OD_{600} was 0.2 in MSM three-fold buffered and 30 mM glucose and 1 mM supplemented precursor benzoate, salicylate or 3-hydroxybenzoate. **B**) Mass balance of benzoate, cinnamate and 2,4,6-TriHBP in medium control, supernatant and total culture extract. Error bars represent standard deviation (n = 4 and n = 3). Abbreviation ND, not detected.

3.4. Mutasynthesis with fluoro-benzoates and methyl-benzoate

The artificial incorporation of fluorine can tune physiochemical features of organic molecules and halogenation also modifies persistence of drugs (Reed & Alper, 2018; Shi et al., 2022). Incorporation of fluorine by PKS III was already demonstrated for flavanones (Abe et al., 2000) and stilbenes (Morita et al., 2001). In order to test weather fluorine can also be incorporated into benzophenones, different fluorobenzoate derivatives were used for polyketide formation (Fig. 4B). Conversion by *P. taiwanensis* GRC3Δ6MC-III with pBT'T plasmids containing different combinations of ligases and BPS or BIS (Fig. 2, Fig. 4B) resulted in 2-F-cinnamate and 2,4,6-trihydroxy-2′-F-benzophenone from 2-F-benzoic acid (see supplementary material). From 3-F-benzoic acid the respective products 3-F-cinnamate and 2,4,6-trihydroxy-3′-F-benzophenone were synthesized (see supplementary material). However, for the fluoro-benzophenone products several signals were observed in LC-MS/MS analysis relating to the expected *m/z* and characteristic fragmentation pattern for identification. This also reveals that several products beside the expected main product were formed which might be related to the previously observed product instability in medium. The fluorinated products had a slightly retarded retention time when compared to their natural pendant likely due to weaker van-der-Waals interaction (Dalvi & Rossky, 2010). Semi-quantitative tendencies (see supplementary material) reveal RpBZL was the preferred ligase compared to $PxBCL_M$ for 2- and 3-F-benzoate derived products. Use of HaBPS resulted in higher 2- or 3-F-cinnamate signals and HsBPS in higher fluorinated polyketide signals respectively which may reflect the BPS promiscuity and binding affinities towards the respective intermediate products during elongation synthesis.

When using 3-methyl benzoate as supplement the respective conversion product 3-methyl cinnamate was detected but not the corresponding methyl trihydroxybenzophenone (Fig. 4 B, see supplementary material) which would result from full conversion by a respective BPS. The highest signals for 3-methyl cinnamate were reached when $PxBCL_M$ was used as ligase in conversions. As a control, samples from cultivations without any supplemented precursor resulted in no product formation and addition of benzoate resulted in cinnamate and 2,4,6-TriHBP formation, as expected.

These qualitative detections of fluorinated products indicate that the used ligases and BPSs can accept fluorinated precursors to some extend and that 3-methyl benzoyl-CoA extension by BPSs and BISs are only incomplete. These findings support the understanding of PKS III promiscuity towards starter units and pave the way for future benzophenone derivatization in bioconversions. Additionally, promiscuity opens new opportunities for fluoro-phenylpropanoid synthesis which might be further improved by engineering enzymatic activity towards their synthesis in future which was already in focus for type I PKS systems (Rittner et al., 2022). The biggest challenge of protein engineering of PKS III will likely be the lack of high throughput screening assays.

3.5. In situ product removal of 2,4,6-TriHBP in two-phase cultivation

Instability of 2,4,6-TriHBP heterologous (hydroxy)benzophenone biosynthesis was previously suggested by Klamrak et al. (2021). A red precipitate was observed when the colored culture supernatant of the toxicity experiment was treated with hydrochloric acid while the liquid remained yellow (Fig. 5A). A pure 2,4,6-TriHBP solution remains clear at low pH. Abiotic 2,4,6-TriHBP degradation experiments in medium with different trace element solutions at low pH (Fig. 5A) led to the assumption that under aerobic conditions, 2,4,6-TriHBP polymerizes to a 'benzoyl-phlorotannin'-like product at moderate pH (>6) and in the presence of iron ions (Wang et al., 2017). According to this hypothesis, iron is either directly reduced from an electron of 2,4,6-TriHBP or from formed radical oxygen species (ROS), subsequently resulting in a phenol coupling reaction (Phang et al., 2023) (see supplementary material), leading to product loss and potential toxic conversion products.

Given that this product instability is a result of deprotonation and metal ions in medium, ISPR with a water-immiscible organic solvent was

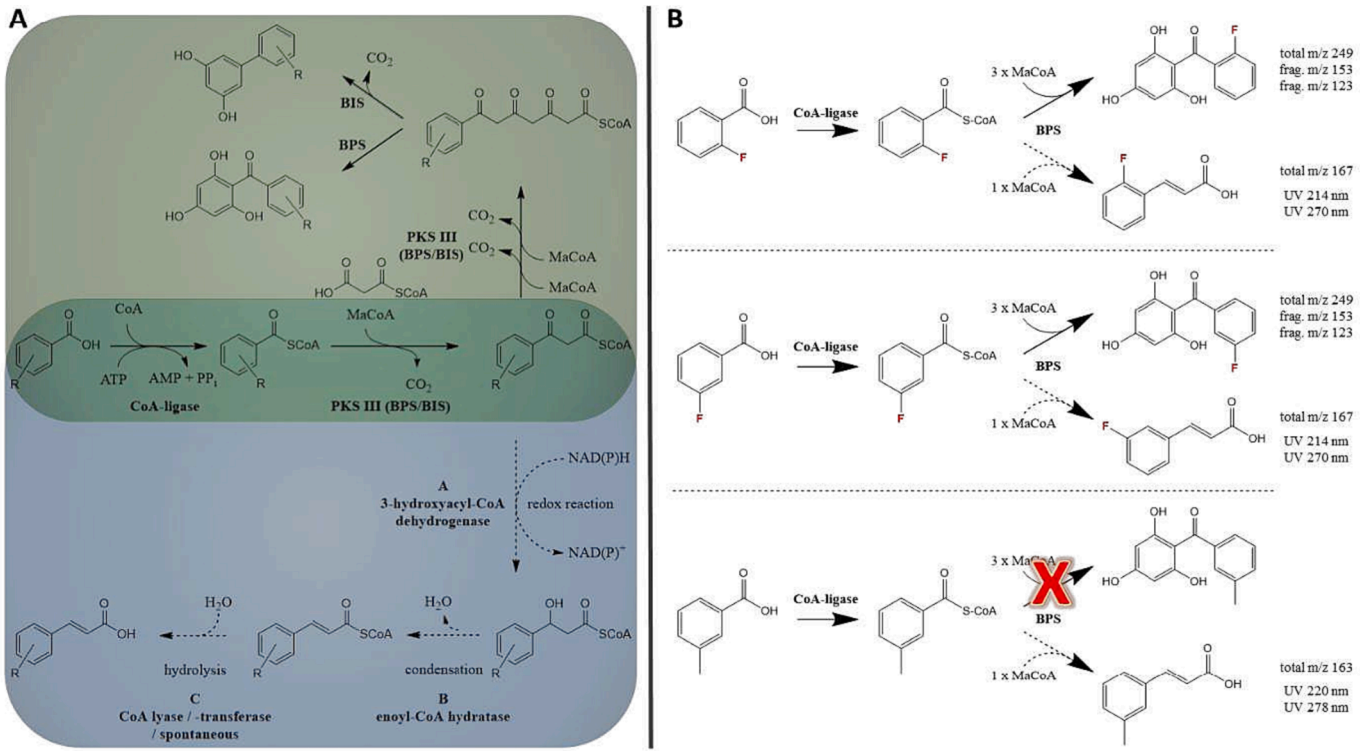

Fig. 4. By-product formation and mutasynthesis. **A)** Schematic reaction of the proposed pathway for phenylpropanoid side-product formation by PKS type III in a heterologous host like *P. taiwanensis* VLB120. Solid arrows indicate polyketide formation reactions (green region). Dashed arrows indicate putative reactions towards phenylpropanoids (blue region) with indications of required reactions A, B and C. CoA release is not indicated in the illustration. **B)** Schematic conversion products from fluorinated or methylated benzoate precursors in mutasynthesis experiments by CoA ligases and BPS. UV spectra maxima and *m/z* in H^+ mode of the molecule and respective signature fragments are given (see supplementary material). Abbreviations: CoA, coenzyme A; MaCoA, malonyl coenzyme A; PKS III, polyketide synthase type III; BPS/BIS, benzophenone synthase / biphenyl synthase; NAD(P)H, nicotinamide adenine dinucleotide (phosphate); frag, signature fragment; UV, ultraviolet.

considered to avoid this effect by sequestering the instable product (Fig. 5B). Such *in situ* liquid–liquid extraction can increase overall product titer and facilitate downstream purification. The concept of two-phase partitioning bioreactors is used in environmental biotechnology for treatment of toxic and/or volatile compounds but it can also be used as reservoir strategy for the product (Heipieper et al., 2007). Many natural products including polyketides exhibit similar physical properties regarding solubility and partitioning into organic solvents from aqueous solutions (Schönsee & Bucheli, 2020). The used biotechnological host organism defines the degree of freedom in the choice of solvents, and the solvent-tolerant *P. taiwanensis* VLB120 used here allows a wide degree of freedom due its native solvent resistance to saturated solutions of 1-octanol, styrene and others (Blombach et al., 2022).

A solvent screening was performed to identify a suitable extractant for *in situ* product removal. An initial pre-selection was done based on physicochemical properties which were: density $\leq$ 900 g L^{-1}; boiling point $\geq$ 120°C; solubility in water $\leq$ 0.3 g L^{-1}; $logP_{O/W} \geq 3.1$; toxicity health score $\leq$ 2 (if available) (Grundtvig et al., 2018) and flash point $\geq$ 95°C. Solvents fulfilling these criteria allow facilitated separation, safe handling, and reduced solvent loss in future applications. Additionally, the low $logP_{O/W}$ boundary takes account of the host's solvent tolerance. This led to the selection of methyl decanoate, ethyl decanoate, dioctyl ether, ethyl oleate, hexadecane, butyl octanoate, isobutyl octanoate, 2-butyl-octanoic acid (CAS 27610-92-0) and 2-hexyldecanoic acid (CAS 25354-97-6) (see supplementary material). Nevertheless, some solvents outside these strict boundaries have a lower flashpoint but a history of previous applications, namely 1-octanol, 1-nonanol, 1-decanol and 2-undecanone (Demling et al., 2020) and were therefore considered as well. These 13 solvents were experimentally tested for their extraction efficiency regarding the product 2,4,6-TriHBP, the by-product cinnamate, the substrate benzoate and the hydrophilic polyketide product flaviolin to evaluate transferability of these results to other applications (see supplementary material). Additional factors such as liquid–liquid phase separation, (see supplementary material), biocompatibility (see supplementary material), and use as sole carbon source by *P. taiwanensis* VLB120 (see supplementary material) were examined.

The five most suitable solvents are shown in Fig. 5C. Partitioning of 2,4,6-TriHBP, benzoate, and cinnamate was best for long chain alcohols (see supplementary material), 2-undecanone and medium-chain-length ester solvents. To consider purification of 2,4,6-TriHBP from benzoate or cinnamate by-product present in culture broth, the separation factor was determined from their respective partitioning coefficients. Phase separation and formation of an undesired interphase was the poorest for the alcohols and the solvents were ranked accordingly (rank 1, poor to rank 5, good) (see supplementary material). Solvents serving as sole carbon source by *P. taiwanensis* VLB120 were also expressed in a ranking from undesired 'good growth' (rank 1) to 'no growth' (rank 5) (see supplementary material). As expected all alcohols were consumed as well as isobutyl octanoate which may indicate some promiscuity of native esterases.

Considering all criteria, 2–undecanone and medium-chain-length esters were the most promising solvents and increasing the stability of externally added 2,4,6-TriHBP (Fig. 5B). Thus, these five candidates were tested in biotransformation approaches using 20%$_{v/v}$ of the respective solvent as *in situ* extractant (Fig. 5D, see supplementary material). These cultures were performed with 30 mM glucose and 1 mM of the respective aromatic precursor, with a starting OD_{600} of 0.2 which is expected to increase to approximately 4 based on online growth measurement. Total 2,4,6-TriHBP titers were approximately doubled from 45 mg·L^{-1} (0.2 mM) to 86.9 mg·L^{-1} (0.378 mM) with 2-undecanone or

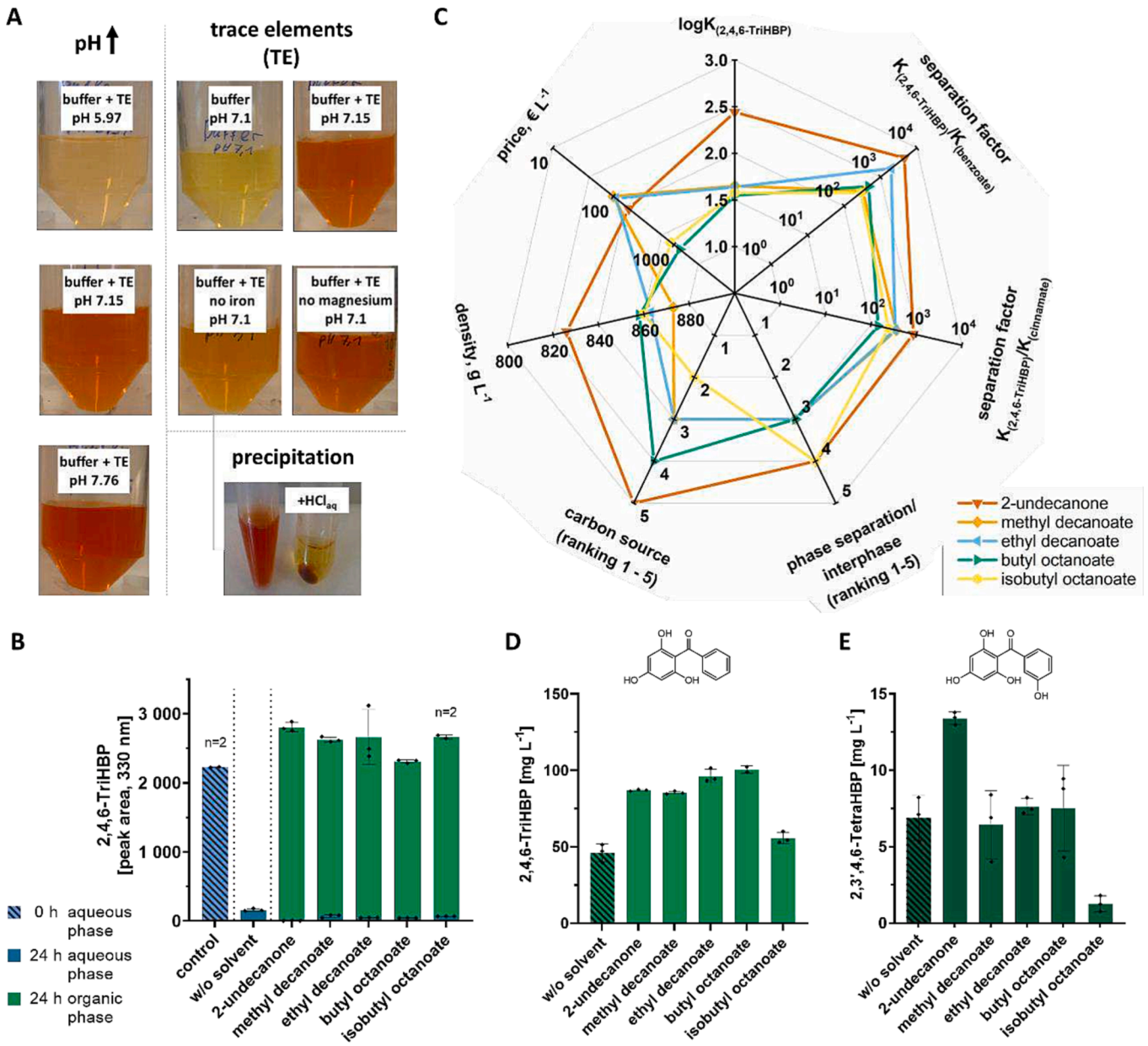

Fig. 5. Polyketide 2,4,6-TriHBP conversion, solvent screening and application. **A)** Images of 2,4,6-TriHBP solutions after 24 h in phosphate buffer (36 mM) with trace elements (TE) at pH 6, 7.2 and 7.8 (left) and with variations of trace element solution with and without Fe and Mg. Precipitation of conversion product in 2,4,6-TriHBP solution in P_i-buffer before and after addition of HCl_{aq} (bottom). **B)** Remaining 2,4,6-TriHBP (from 1 mM) in MSM with and without a 2:1 ratio of solvent after 24 h. **C)** Radar chart of selected solvent screening parameters and selected solvents (see supplementary material for all considered parameters and solvents in experimental screening procedure). **D)** Titer of 2,4,6-TriHBP and **E)** 2,3′,4,6-TetraHBP in two-phase cultivations from bioconversion by strain GRC3Δ6MC-II pBT'T-HsBPS-RpBZL in three-fold buffered MSM (+Km) 30 mM glucose and 2 mM supplemented benzoate or 3-hydroxybenzoate and 20% solvent, respectively. Inoculation occurred with calculated OD_{600} of 0.2. Error bars represent the standard deviations after 24 h (n = 3, if not indicated differently). Abbreviation: w/o, without.

even 100.4 mg L^{-1} (0.436 mM) with butyl octanoate as solvent phase. However, this was not the case for isobutyl octanoate, in spite of the fact that the latter served as potential additional carbon source. Hence, product concentration within the organic solvent were approximately 2 mM in 2-undecanone. In principle, back-extraction of 2,4,6-TriHBP from 2-undecanone solution can be achieved by an alkaline solution at pH 12 with about 71% efficiency (see supplementary material).

When using 3-hydroxybenzoate for the 2,3′,4,6-TetraHBP production only 2-undecanone increased total product titers from 6.9 ± 1.5 mg L^{-1} (0.028 mM) to 13.4 ± 0.4 mg L^{-1} (0.054 mM) (Fig. 5E). According to these results, 2-undecanone was the most suitable solvent for *in situ* polyketide extraction. The benefit of using a solvent-tolerant *Pseudomonas* is apparent in direct comparison to different microbes in two-phase cultivations with 2-undecanone, especially compared to yeast or Gram-positive bacteria (see supplementary material), which was expected due to 2-undecanone's $logP_{O/W}$ of 4.1.

In order to test whether the addition of solvents *per se* can affect polyketide formation, flaviolin as a highly hydrophilic product deriving from malonyl-CoA condensation was produced. Here, no effect was observed for most solvents as expected except for 2-undecanone which even reduced flaviolin titers (see supplementary material). This may be due to structural similarities of the solvent with intermediate condensation products leading to enzyme inhibition by competition. Overall, these results demonstrate the benefit of ISPR for reducing product instability and inhibition. Additionally, it highlights the need to tailor solvent screenings to product, substrate, and microbes accordingly.

3.6. Heterologous de novo polyketide synthesis in solvent two-phase cultivation

The supplementation of aromatic precursors for polyketide starter units represents an additional production parameter that increases cost and process complexity and may hinder commercialization as "natural-origin" product. To circumvent this, production modules for benzoate (*attTn7*::*FRT-P*$_{14f}$-*phdBCDE-Sc4CL-AtPAL2*) (Otto et al., 2020), 3-hydroxybenzoate (*attTn7*::*P*$_{14f}$-*LaCH-II*), and 2-hydroxybenzoate (*attTn7*::*P*$_{14g}$-*menF-pchB*) were constructed and genomically integrated into the malonyl-CoA platform strain GRC3Δ6MC-III with increased malonyl-CoA availability (Schwanemann et al., 2023). The resulting strains were subsequently transformed with pBT'T-based plasmids for the *de novo* synthesis of 2,4,6-TriHBP, 3,5-dihydroxybiphenyl, 2,3',4,6-TetraHBP or 4-hydroxycoumarin. These strains were able to produce the target polyketide fully *de novo*, i.e., in a mineral glucose medium with 2-undecanone for ISPR without supplementation of aromatic precursors. Thus, it is in principle possible to produce them from sustainable resources including the solvent 2-undecanone (Nies et al., 2020). For 2,4,6-TriHBP, 3,5-dihydroxybiphenyl and 2,3',4,6-TetraHBP this represents their first heterologous *de novo* biosynthesis.

As before, the highest titers were achieved with 2,4,6-TriHBP, indicating that in this *de novo* biosynthesis the polyketide production module is the limiting factor. The best producing strains of GRC3Δ6MC-III *attTn7*::*FRT-P*$_{14f}$-*phdBCDE-sc4CL-atPAL2* pBT'T-*HsBPS-RpBZL* produced 17.9 ± 0.14 mg L^{-1} 2,4,6-TriHBP from 30 mM glucose (Fig. 6A) which is about a third of what was produced in previous biotransformation approaches (Fig. 3). The challenging competition for carbon between malonyl-CoA and products of the shikimate pathway needed in polyketide formation were already revealed during construction of the GRC3Δ6MC-III strain (Schwanemann et al., 2023). Clonal variation from different transformants was observed for two out of six 2,4,6-TriHBP production strains, as well as for other producers which indicates genetic instability of the combined production modules. However, error margins between replicates of single transformants were small and not significant, enabling reliable production from selected clones. Benzoate formation is a result of the incorporated phenylalanine ammonia-lyase together with the phenylpropanoid degradation pathway that converts cinnamate to benzoate. The well-performing clones produced no cinnamate, while this intermediate was detected in cultures with low 2,4,6-TriHBP titers, suggesting a bottleneck at the level of *phdBCDE* in the latter strains.

Titers of 3,5-dihydroxybiphenyl by strain GRC3Δ6MC-III *attTn7*::*FRT-P*$_{14f}$-*phdBCDE-sc4CL-atPAL2* pBT'T-*MdBIS1-RpBZL* were around 0.75 mg L^{-1} (Fig. 6B). Concentrations of benzoate were about three-fold higher (0.15 mM) than in the 2,4,6-TriHBP cultures and no cinnamate was detected. This represents the first heterologous *de novo* 3,5-dihydroxybiphenyl biosynthesis, while the relatively low titers highlight the potential of engineering BIS kinetics applicable in biotechnological productions.

With the 2,3′,4,6-TetraHBP production strain, titers of approximately 1.6 mg L^{-1} were achieved without significant differences between tested clones (Fig. 6C). In this strain, the 3-hydroxybenzoate precursor is synthesized via a chorismatase type II enzyme from *Lentzea aerocolonigenes* (LaCH-II, see supplementary material) (Grüninger et al., 2019). This one-step synthesis of 3-hydroxybenzoate from chorismate resulted in much higher precursor titers up to 0.55 mM, even though this strain is not engineered in its shikimate pathway. Interestingly, the concentration of this PKS-synthesized by-product 3-hydroxycinnamate (2.5 mg L^{-1}) was higher than that of the main product 2,3′,4,6-TetraHBP, again highlighting the *in vivo* drain of polyketide intermediates as described above in the biotransformation experiments. This is likely a result of disadvantageous BPS kinetics to alternative starting substrates in combination with increased K_M for malonyl-CoA extender units for alternative starters (Chizzali et al., 2016; Huang et al., 2012). Identification of a specific BPS sequence for 3-hydroxybenzoyl-CoA, plus deletion of β-oxidation genes responsible for PKS-intermediate conversion may thus improve heterologous 2,3′,4,6-TetraHBP synthesis.

4-Hydroxycoumarin synthesis requires 2-hydroxybenzoate formation from chorismate in two-steps by an isochorismate synthase (menF,

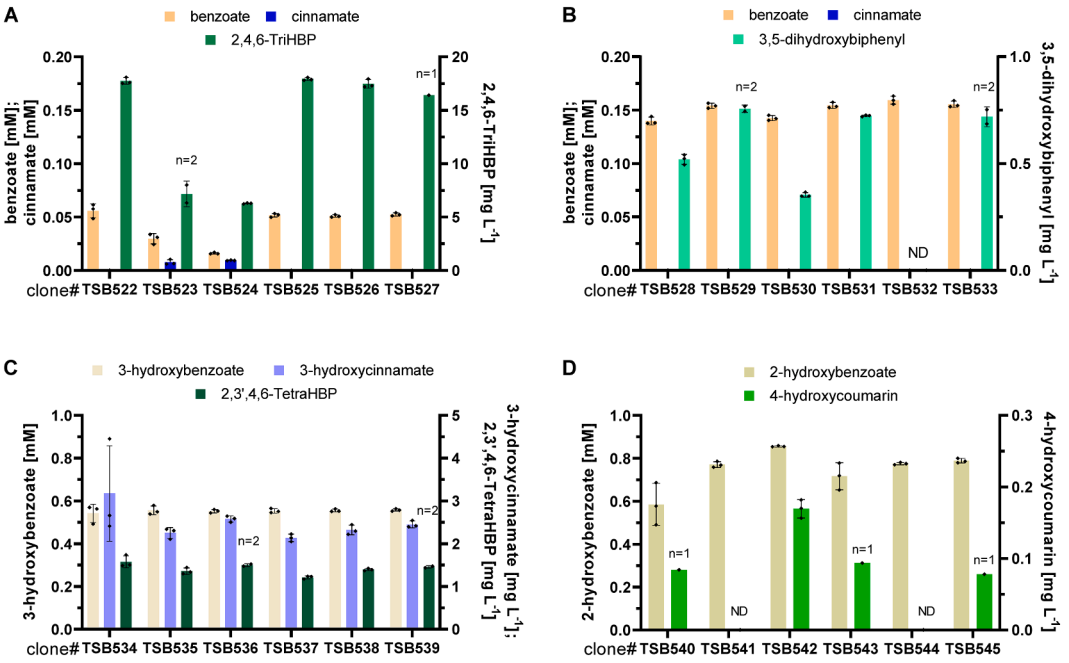

Fig. 6. Two-phase cultivation for *de novo* product biosynthesis. **A)** Titers of benzoate, cinnamate and 2,4,6-TriHBP from strain GRC3Δ6MC-III *attTn7*::*FRT-P*$_{14f}$-*phdBCDE-sc4CL-atPAL2* pBT'T-*HsBPS-RpBZL*; **B)** titers of benzoate, cinnamate and 3,5-dihydroxybiphenyl from strain GRC3Δ6MC-III *attTn7*::*FRT-P*$_{14f}$-*phdBCDE-sc4CL-atPAL2* pBT'T-*MdBIS1-RpBZL*; **C)** titers of 3-hydroxybenzoate, 3-hydroxycinnamate and 2,3′,4,6-TetraHBP from strain GRC3Δ6MC-III *attTn7*::*P*$_{14f}$-*LaCH-II* pBT'T-*HsBPS-RpBZL*; **D)** titers of 2-hydroxycinnamate and 4–hydroxycoumarin from strain GRC3Δ6MC-III *attTn7*::*P*$_{14g}$-*menF-pchB* pBT'T-*PcBIS1-sdgA* from 30 mM glucose in *de novo* biosynthesis in two-phase cultivation with 20% (v/v) solvent. Error bars represent standard deviation of three replicates (n = 3) if not indicated differently. Abbreviation: ND, not detected; TSB522-545, individual strain number. Significance was determined by two-way ANOVA with tukey test.

see supplementary material) and isochorismate pyruvate lyase (pchB, see supplementary material). Up to 0.85 mM 2-hydroxybenzoate were produced by strain GRC3Δ6MC-III *attTn7*::P_{14f}-*menF-pchB* pBT'T-*PcBIS1-sdgA* (Fig. 6D) revealing dependency on used precursor production modules. Exploiting biphenyl synthase side-activity for salicyl-CoA conversion product was inefficient because product titers, if obtained any, were close to the detection limit to allow characteristic UV spectra and reached up to 0.17 mg L^{-1} 4-hydroxycoumarin. Nevertheless, the successful *de novo* 4-hydroxycoumarin synthesis by biphenyl synthases demonstrates the broad applicability of BIS (Liu et al., 2010) as an alternative to other already established synthesis routes (Lin et al., 2013).

A combination of genetic modules for polyketide and precursor synthesis enabled completely *de novo* production from glucose, but the relatively low product titers compared to cultures with supplementation of benzoate, 3-hydroxybenzoate or 2-hydroxybenzoate will likely make the biotransformation approach more efficient. Further evaluation is needed here with regard to process intensifications including higher substrate and biomass concentrations to boost product titers.

4. Conclusion

This study achieved microbial synthesis of plant-benzophenones, 3,5-dihydroxybiphenyl, and 4-hydroxycoumarin. *P. taiwanensis* GRC3Δ6 MC-III proved an efficient host, thriving in two-phase cultivations with 2-undecanone for ISPR to enhance product titers and stability. Mutasynthesis approaches enabled the proof-of-principle production of methylated and fluorinated polyketides, which may be further increased if PKS can be tailored to the specific precursors. In summary, this study establishes a versatile *Pseudomonas* production platform in an aqueous-organic two-phase cultivation for the synthesis of polyketides with a broad application range, which can be further enhanced by process intensification, and expanded by the implementation of new precursor-pathway combinations.

CRediT authorship contribution statement

Tobias Schwanemann: Conceptualization, Methodology, Validation, Formal analysis, Investigation, Writing – original draft, Visualization, Funding acquisition. **Esther A. Urban:** Methodology, Formal analysis, Investigation. **Christian Eberlein:** Methodology, Formal analysis. **Jochem Gätgens:** Methodology, Formal analysis. **Daniela Rago:** Methodology, Formal analysis. **Nicolas Krink:** Supervision, Writing – review & editing. **Pablo I. Nikel:** Conceptualization, Resources, Writing – review & editing. **Hermann J. Heipieper:** Resources. **Benedikt Wynands:** Validation, Writing – review & editing, Supervision. **Nick Wierckx:** Conceptualization, Validation, Resources, Writing – review & editing, Supervision, Funding acquisition, Project administration.

Declaration of Competing Interest

The authors declare that they have no known competing financial interests or personal relationships that could have appeared to influence the work reported in this paper.

Data availability

Data will be made available on request.

Acknowledgements

The authors are thankful to Prof. Ludger Beerhues and Dr. Benye Liu from the Institute of Pharmaceutical Biology at Technical University of Braunschweig for their kind gifts of plasmids containing RpBZL, HaBPS, HsBPS and SaBIS1 and to provide reference UV spectra of products, as well as for fruitful scientific discussions. Additionally, TS is thankful to Julian Greb for discussions and input about the 2,4,6-TriHBP polymerization hypothesis.

Funding

T.S. gratefully acknowledges the support by the German Federal Environmental Foundation (DBU) [PhD Scholarship 20019/638-32] and German Academic Exchange Service (DAAD) [scholarship 57556281]; C.E., H.H., B.W. and N.W. thank the German Federal Ministry of Education and Research (BMBF) with the project NO-STRESS [FKZ 031B0852A and 031B0852C]. NW further acknowledges funding from the European Union (ERC, PROSPER, 101044949). The financial support from The Novo Nordisk Foundation through grants NNF20CC0035580, LiFe (NNF18OC0034818) and TARGET (NNF21OC0067996), the Danish Council for Independent Research (SWEET, DFF-Research Project 8021-00039B), and the European Union's Horizon 2020 Research and Innovation Programme under grant agreement No. 814418 (SinFonia) to P.I.N. is gratefully acknowledged. N.K. gratefully acknowledges the support of the Novo Nordisk Foundation Postdoctoral Fellowship for research within biotechnology-based synthesis and production: DF2AP2 (NNF20OC0065068).

Appendix A. Supplementary data

Supplementary data to this article can be found online at https://doi.org/10.1016/j.biortech.2023.129741.

References

Abe, I., Morita, H., Nomura, A., Noguchi, H., 2000. Substrate specificity of chalcone synthase: Enzymatic formation of unnatural polyketides from synthetic cinnamoyl-CoA analogues. J. Am. Chem. Soc. 122 (45), 11242–11243. https://doi.org/10.1021/ja0027113.

Beerhues, L., Liu, B., 2009. Biosynthesis of biphenyls and benzophenones - Evolution of benzoic acid-specific type III polyketide synthases in plants. Phytochemistry 70 (15–16), 1719–1727. https://doi.org/10.1016/j.phytochem.2009.06.017.

Bisht, R., Bhattacharyya, A., Shrivastava, A., Saxena, P., 2021. An Overview of the Medicinally Important Plant Type III PKS Derived Polyketides. Front. Plant Sci. 12 (October), 1–21. https://doi.org/10.3389/fpls.2021.746908.

Bligh, E.G., Dyer, W.J., 1959. A rapid method of total lipid extraction and purification. Can. J. Biochem. Physiol. 37 (8).

Blombach, B., Grünberger, A., Centler, F., Wierckx, N., Schmid, J., 2022. Exploiting unconventional prokaryotic hosts for industrial biotechnology. Trends Biotechnol. 40 (4), 385–397. https://doi.org/10.1016/j.tibtech.2021.08.003.

Chizzali, C., Swiddan, A.K., Abdelaziz, S., Gaid, M., Richter, K., Fischer, T.C., Liu, B., Beerhues, L., 2016. Expression of biphenyl synthase genes and formation of phytoalexin compounds in three fire blight-infected *Pyrus communis* cultivars. PLoS One 11 (7), 1–16. https://doi.org/10.1371/journal.pone.0158713.

Choo, H.J., Ahn, J.H., 2019. Synthesis of Three Bioactive Aromatic Compounds by Introducing Polyketide Synthase Genes into Engineered *Escherichia coli*. J. Agric. Food Chem. 67 (31), 8581–8589. https://doi.org/10.1021/acs.jafc.9b03439.

Cros, A., Alfaro-Espinoza, G., Maria, A.D., Wirth, N.T., Nikel, P.I., 2022. Synthetic metabolism for biohalogenation. Curr. Opin. Biotechnol. 74, 180–193. https://doi.org/10.1016/j.copbio.2021.11.009.

Dalvi, V. H., & Rossky, P. J. (2010). Molecular origins of fluorocarbon hydrophobicity. Proceed. Natl. Acad. Sci. United States of America, *107*(31), 13603–13607. https://doi.org/10.1073/pnas.0915169107.

Demling, P., von Campenhausen, M., Grütering, C., Tiso, T., Jupke, A., Blank, L.M., 2020. Selection of a recyclable *in situ* liquid-liquid extraction solvent for foam-free synthesis of rhamnolipids in a two-phase fermentation. Green Chem. 22, 8495–8510. https://doi.org/10.1039/D0GC02885A.

Eberlein, C., Baumgarten, T., Starke, S., Heipieper, H.J., 2018. Immediate response mechanisms of Gram-negative solvent-tolerant bacteria to cope with environmental stress: *cis-trans* isomerization of unsaturated fatty acids and outer membrane vesicle secretion. Appl. Microbiol. Biotechnol. 102 (6), 2583–2593. https://doi.org/10.1007/s00253-018-8832-9.

Ehianeta, T.S., Laval, S., Yu, B., 2016. Bio- and chemical syntheses of mangiferin and congeners. Biofactors 42 (5), 445–458. https://doi.org/10.1002/biof.1279.

Grundtvig, I.P.R., Heintz, S., Krühne, U., Gernaey, K.V., Adlercreutz, P., Hayler, J.D., Wells, A.S., Woodley, J.M., 2018. Screening of organic solvents for bioprocesses using aqueous-organic two-phase systems. Biotechnol. Adv. 36 (7), 1801–1814. https://doi.org/10.1016/j.biotechadv.2018.05.007.

Grüninger, M.J., Buchholz, P.C.F., Mordhorst, S., Strack, P., Müller, M., Hubrich, F., Pleiss, J., Andexer, J.N., 2019. Chorismatases-the family is growing. Org. Biomol. Chem. 17 (8), 2092–2098. https://doi.org/10.1039/c8ob03038c.

Heipieper, H.J., Diefenbach, R., Keweloh, H., 1992. Conversion of *cis* unsaturated fatty acids to *trans*, a possible mechanism for the protection of phenol-degrading *Pseudomonas putida* P8 from substrate toxicity. Appl. Environ. Microbiol. 58 (6), 1847–1852. https://doi.org/10.1128/aem.58.6.1847-1852.1992.

Heipieper, H.J., Neumann, G., Cornelissen, S., Meinhardt, F., 2007. Solvent-tolerant bacteria for biotransformations in two-phase fermentation systems. Appl. Microbiol. Biotechnol. 74 (5), 961–973. https://doi.org/10.1007/s00253-006-0833-4.

Huang, L., Wang, H., Ye, H., Du, Z., Zhang, Y., Beerhues, L., Liu, B., 2012. Differential Expression of Benzophenone Synthase and Chalcone Synthase in *Hypericum sampsonii*. Nat. Prod. Commun. 7 (12), 1615–1618. https://doi.org/10.1177/1934578x1200701219.

Hummel, J., Strehmel, N., Selbig, J., Walther, D., Kopka, J., 2010. Decision tree supported substructure prediction of metabolites from GC-MS profiles. Metabolomics 6 (2), 322–333. https://doi.org/10.1007/s11306-010-0198-7.

Isogai, S., Tominaga, M., Kondo, A., Ishii, J., 2022. Plant Flavonoid Production in Bacteria and Yeasts. Front. Chem. Eng. 4 (July), 1–20. https://doi.org/10.3389/fceng.2022.880694.

Kallscheuer, N., Polen, T., Bott, M., Marienhagen, J., 2017. Reversal of β-oxidative pathways for the microbial production of chemicals and polymer building blocks. Metab. Eng. 42 (May), 33–42. https://doi.org/10.1016/j.ymben.2017.05.004.

Kallscheuer, N., Classen, T., Drepper, T., Marienhagen, J., 2019. Production of plant metabolites with applications in the food industry using engineered microorganisms. Curr. Opin. Biotechnol. 56, 7–17. https://doi.org/10.1016/j.copbio.2018.07.008.

Kildegaard, K.R., Arnesen, J.A., Adiego-Pérez, B., Rago, D., Kristensen, M., Klitgaard, A. K., Hansen, E.H., Hansen, J., Borodina, I., 2021. Tailored biosynthesis of gibberellin plant hormones in yeast. Metab. Eng. 66 (February), 1–11. https://doi.org/10.1016/j.ymben.2021.03.010.

Klamrak, A., Nabnueangsap, J., Nualkaew, N., 2021. Biotransformation of Benzoate to 2,4,6-Trihydroxybenzophenone by Engineered *Escherichia coli*. Molecules 26 (9), 2779. https://doi.org/10.3390/molecules26092779.

Li, H., Lyv, Y., Zhou, S., Yu, S., Zhou, J., 2022. Microbial cell factories for the production of flavonoids–barriers and opportunities. Bioresour. Technol. 360, 127538. https://linkinghub.elsevier.com/retrieve/pii/S0960852422008677.

Lin, Y., Shen, X., Yuan, Q., Yan, Y., 2013. Microbial biosynthesis of the anticoagulant precursor 4-hydroxycoumarin. Nat. Commun. 4 (May), 1–8. https://doi.org/10.1038/ncomms3603.

Liu, B., Kalz, L.F., Jia, Y., Grull, M., Beuerle, T., Beerhues, L.. Engineering yeast for production of benzophenones and xanthones as precursors of polycyclic polyprenylated acylphloroglucinols. https://doi.org/10.24355/dbbs.084-202001221215-0.

Liu, B., Raeth, T., Beuerle, T., Beerhues, L., 2007. Biphenyl synthase, a novel type III polyketide synthase. Planta 225 (6), 1495–1503. https://doi.org/10.1007/s00425-006-0435-5.

Liu, B., Raeth, T., Beuerle, T., Beerhues, L., 2010. A novel 4-hydroxycoumarin biosynthetic pathway. Plant Mol. Biol. 72 (1–2), 17–25. https://doi.org/10.1007/s11103-009-9548-0.

Miller, N., Malherbe, C.J., Joubert, E., 2020. Xanthone- and benzophenone-enriched nutraceutical: Development of a scalable fractionation process and effect of batch-to-batch variation of the raw material (Cyclopia genistoides). Sep. Purif. Technol. 237, 116465 https://doi.org/10.1016/J.SEPPUR.2019.116465.

Morita, H., Noguchi, H., Schröder, J., Abe, I., 2001. Novel polyketides synthesized with a higher plant stilbene synthase. Eur. J. Biochem. 268 (13), 3759–3766. https://doi.org/10.1046/j.1432-1327.2001.02289.x.

Morita, H., Wong, C.P., Abe, I., 2019. How structural subtleties lead to molecular diversity for the type III polyketide synthases. J. Biol. Chem. 294 (41), 15121–15136. https://doi.org/10.1074/jbc.REV119.006129.

Nies, S.C., Alter, T.B., Nölting, S., Thiery, S., Phan, A.N.T., 2020. High titer methyl ketone production with tailored *Pseudomonas taiwanensis* VLB120. Metab. Eng. 62, 84–94. https://doi.org/10.1016/j.ymben.2020.08.003.

Nualkaew, N., Morita, H., Shimokawa, Y., Kinjo, K., Kushiro, T., De-Eknamkul, W., Ebizuka, Y., Abe, I., 2012. Benzophenone synthase from *Garcinia mangostana* L. pericarps. Phytochemistry 77, 60–69. https://doi.org/10.1016/j.phytochem.2012.02.002.

Otto, M., Wynands, B., Marienhagen, J., Blank, L.M., Wierckx, N., 2020. Benzoate Synthesis from Glucose Or Glycerol Using Engineered *Pseudomonas taiwanensis*. Biotechnol. J. 2000211, 2000211. https://doi.org/10.1002/biot.202000211.

Phang, S.J., Teh, H.X., Looi, M.L., Arumugam, B., Fauzi, M.B., Kuppusamy, U.R., 2023. Phlorotannins from brown algae: a review on their antioxidant mechanisms and applications in oxidative stress-mediated diseases. J. Appl. Phycol. 0123456789 https://doi.org/10.1007/s10811-023-02913-4.

Prabowo, C.P.S., Eun, H., Yang, D., Huccetogullari, D., Jegadeesh, R., Kim, S.J., Lee, S.Y., 2022. Production of natural colorants by metabolically engineered microorganisms. Trend. Chem. 4 (7), 608–626. https://doi.org/10.1016/J.TRECHM.2022.04.009.

Reed, K.B., Alper, H.S., 2018. Expanding beyond canonical metabolism: Interfacing alternative elements, synthetic biology, and metabolic engineering. Synth. Syst. Biotechnol. 3 (1), 20–33. https://doi.org/10.1016/j.synbio.2017.12.002.

Remali, J., Sahidin, I., Aizat, W.M., 2022. Xanthone Biosynthetic Pathway in Plants: A Review. Front. Plant Sci. 13 (April), 1–15. https://doi.org/10.3389/fpls.2022.809497.

Rittner, A., Joppe, M., Schmidt, J.J., Mayer, L.M., Reiners, S., Heid, E., Herzberg, D., Sherman, D.H., Grininger, M., 2022. Chemoenzymatic synthesis of fluorinated polyketides. Nat. Chem. 14 (9), 1000–1006. https://doi.org/10.1038/s41557-022-00996-z.

Schönsee, C.D., Bucheli, T.D., 2020. Experimental Determination of Octanol-Water Partition Coefficients of Selected Natural Toxins. J. Chem. Eng. Data 65 (4), 1946–1953. https://doi.org/10.1021/acs.jced.9b01129.

Schwanemann, T., Otto, M., Wierckx, N., Wynands, B., 2020. *Pseudomonas* as Versatile Aromatics Cell Factory. Biotechnol. J. 1900569, 1900569. https://doi.org/10.1002/biot.201900569.

Schwanemann, T., Otto, M., Wynands, B., Marienhagen, J., Wierckx, N., 2023. A *Pseudomonas taiwanensis* malonyl-CoA platform strain for polyketide synthesis. Metab. Eng. 77 (February), 219–230. https://doi.org/10.1016/j.ymben.2023.04.001.

Shi, S., Tian, J., Luo, Y., 2022. Recent advances in fluorinated products biosynthesis. Bioresource Technology Reports 20, 101288. https://doi.org/10.1016/j.biteb.2022.101288.

Stewart, C., Woods, K., Macias, G., Allan, A.C., Hellens, R.P., Noel, J.P., 2017. Molecular architectures of benzoic acid-specific type III polyketide synthases. Acta Crystallographica Section D: Structural Biology 73 (12), 1007–1019. https://doi.org/10.1107/S2059798317016618.

Thompson, M.G., Incha, M.R., Pearson, A.N., Schmidt, M., Sharpless, W.A., Eiben, C.B., Cruz-Morales, P., Blake-Hedges, J.M., Liu, Y., Adams, C.A., Haushalter, R.W., Krishna, R.N., Lichtner, P., Blank, L.M., Mukhopadhyay, A., Deutschbauer, A.M., Shih, P.M., Keasling, J.D., 2020. Fatty Acid and Alcohol Metabolism in *Pseudomonas putida*: Functional Analysis Using Random Barcode Transposon Sequencing. Appl. Environ. Microbiol. 86 (21), 1–23. https://doi.org/10.1128/AEM.01665-20.

Virklund, A., Jensen, S. I., Nielsen, A. T., & Woodley, J. M. (2022). Combining genetic engineering and bioprocess concepts for improved phenylpropanoid production. *Biotechnology and Bioengineering*, *November*, 1–16. https://doi.org/10.1002/bit.28292.

Wang, Y., Lin, X., Shao, Z., Shan, D., Li, G., Irini, A., 2017. Comparison of Fenton, UV-Fenton and nano-Fe3O4 catalyzed UV-Fenton in degradation of phloroglucinol under neutral and alkaline conditions: Role of complexation of Fe3+ with hydroxyl group in phloroglucinol. Chem. Eng. J. 313, 938–945. https://doi.org/10.1016/j.cej.2016.10.133.

Wu, S.B., Long, C., Kennelly, E.J., 2014. Structural diversity and bioactivities of natural benzophenones. Nat. Prod. Rep. 31 (9), 1158–1174. https://doi.org/10.1039/c4np00027g.

Wynands, B., Otto, M., Runge, N., Preckel, S., Polen, T., Blank, L.M., Wierckx, N., 2019. Streamlined *Pseudomonas taiwanensis* VLB120 Chassis Strains with Improved Bioprocess Features. ACS Synth. Biol. 8 (9), 2036–2050. https://doi.org/10.1021/acssynbio.9b00108.

Wynands, B., Kofler, F., Sieberichs, A., Silva, N., Wierckx, N., 2023. Engineering a *Pseudomonas taiwanensis* 4-coumarate platform for production of *para*-hydroxy aromatics with high yield and specificity. Metab. Eng. 78, 115–127. https://doi.org/10.1016/j.ymben.2023.05.004.